Materials Research Proceedings 44 (2024) 158-166 https://doi.org/10.21741/9781644903254-18

Material flow analysis in friction stir consolidation during recycling aluminum alloy chips

LATIF Abdul[1,a *], PULEO Riccardo[1,b], INGARAO Giuseppe[1,c], MICARI Fabrizio[1,d] and FRATINI Livan[1,e]

[1]Department of Engineering, University of Palermo, Viale delle Scienze, Palermo, 90128, Italy

[a]abdul.latif@unipa.it, [b]riccardo.puleo01@unipa.it, [c]Giuseppe.ingarao@unipa.it, [d]fabrizio.micari@unipa.it, [e]livan.fratini@unipa.it

Keywords: Friction Stir Consolidation, Recycling, Material Flow, Aluminum Alloys

Abstract. Friction stir consolidation (FSC) is a solid-state process primarily employed to recycle aluminum machining scrap with the aim to meet the increasing demand of aluminum within the framework of sustainability goals. This technology has recently drawn the attention of many researchers due to its potential beyond the recycling approach to offer plausible new routes for alloying and upcycling metal scraps. Concerning the FSC process, a rotating tool with a certain force is applied to a given batch of chips mass enclosed inside a die chamber turning it into a consolidated billet by friction and stirring action of the tool. The obtained samples are characterized by non-homogenous properties as the non-symmetric nature of the process and therefore different strain levels occur while producing the recycled billet. This study was focused on developing a proper experimental setup to visualize material flow supported with preliminary numerical simulation. The adopted approach led to reveal the deformation during the FSC process in different billet regions by visualizing the shape change of the pre-embedded copper marker in the billet.

Introduction

Exploring sustainable recycling processes is the hot trend of the modern world in order to meet the increasing demand for aluminum for various industrial applications in a more sustainable way [1]. Conventionally recycling is performed by re-melting the scraps and transforming them into new products. However, the process itself has several limitations especially when dealing with scraps that have a higher surface area to volume ratio such as machining chips that are produced during manufacturing processes. Such kind of scraps have a higher affinity toward oxidation and therefore lead to higher material loss [2]. Thus, recycling such kinds of scraps by conventional remelting route is neither energy nor resource efficient.

Researchers are continuously exploring solid state techniques for recycling machining chips. These methods outperformed conventional remelting by turning input scraps into semi-finished or finished products by mechanical means or plastic deformation without undergoing the remelting phase. These methods are further categorized into powder metallurgy-based processes such as plasma sintering and plastic deformation-based processes like equal angle channel angle pressing, hot-pressing, high-pressure torsion, and variants of friction stir processing [3].

Recently friction-based solid-state processes such as friction stir welding and its variants like friction stir extrusion, friction stir deposition, and friction consolidation have drawn the attention of many researchers [4-6]. They offer flexibility ranging from welding metals parts to the recycling of the machining scraps. Concerning the field variables of these friction stir processes, it is important to study strain and strain rate, so the microstructure and material properties of the product can be understood and manipulated by varying the process parameters.

The most popular technique adopted by the researchers is inserting a marker in the form of copper or aluminium wire/foil inside the workpiece during the friction stir process. The actual deformation was then obtained by analyzing the deformation of the marker. In this regard, Fratini et al [7] investigated the material flow by analyzing the deformation state of a thin foil embedded at the adjoining edges of AA7075-T6 butt joint during the friction stir welding process. They observed that the material flow on the back of the tool, from the retreating side towards the advancing, is favoring bonding occurrence at the advancing side. Moreover, it worth mentioning that the process parameters, as well as the tool shape, affect the material flow. A qualitative approach was also applied by Seidel and Reynolds using the marker insert technique in FSW to visualize the material flow path after the tool had passed through the workpiece [8].

Friction stir deposition is a variant of the friction stir welding process which involves a layer-by-layer tool deposition to generate multiple metal substrates. Stubblefield et al. [9] developed a combined computational and experimental method for analyzing material flow during the FSD process by embedding a copper wire as a marker inside a AA6061-T6 feedstock. They observed copper particles on the advancing side that were found similar to what Fratini at al [7] observed during FSW.

Friction extrusion is also one of the process categories of FSW that generates large plastic strains and deformation through friction between a rotating die and the material to be extruded. Li et al. [10] developed an experimental approach to get an insight view on strain and strain rate in the FE process and their correlation with process parameters. In specific, they studied the material flow to determine the distribution of steady-state strain and strain rate in friction extrusion by analyzing the shape changes of the deforming markers.

Like FSE, the friction stir consolidation process belongs to the same friction stir welding process category. The process involves a rotating tool, which also applies a vertical load, for compacting and consolidating input chip-mass enclosed inside the die chamber [6]. The heat is generated due to the combined effect of the vertical load and the friction between the tool and the chips, allowing the chips to bond together [11]. The evolution of different process variables such as strain and strain rate are still unknown and are important to predict the properties of final consolidated products.

Therefore, this research is focused on analyzing material flow during the FSC process by using a cooper marker. The strain distribution is quantified considering the geometry change of the marker at a different position in the FSC billet. A full map of material flow in the friction stir consolidation process is determined and presented. In addition, a numerical simulation is performed, and a qualitative comparison is established between the numerical results and the experimental results. In fact, in shaping and forming processes like FSC, it is vital to understand the evolution of microstructure and other material properties with varying process parameters by obtaining the strain and strain rate.

Methodology

A 3 mm thick rolled sheet of AA7075 with average values of 150 HV and 155 μm for hardness and grain size, respectively, was turned into machining scraps through milling operations with tool rotational speed of 1250 rpm, feed rate of 280 mm/min, and cutting depth of 1 mm. FSC process was performed using ESAB LEGIO, a dedicated friction stir welding machine (Fig.1a). The chips were loaded inside the die chamber of H13 steel with a nominal diameter of 25 mm, and an H13 steel tool was employed to compact the chips. A preliminary consolidation step was applied by activating the tool rotation at 1500 rpm with a pressing force starting from 5 kN to 20 kN with 0.5 kN/s increment. Then a hole with a nominal diameter of 1 mm was drilled inside the partially consolidated billet and a copper wire of 1 mm diameter with height equal to the height of the billet (10 mm) was inserted inside the hole as a marker (Fig.1b,c and d). Copper has good ductility with good sensitivity to external deformation and therefore it has been utilized for studying the material

flow in friction stir processing [7]. In order to ensure the precise location of the hole, the drill bit was guided by an auxiliary billet with a hole at a distance of 6.5 mm (1/2r) as shown in Fig. 1d. Then the billet was fully consolidated by applying a rotational speed of 1500 rpm and 20 kN pressing load to the tool for a processing time of 60 s.

After cooling the equipment, the billet was detached from the die and its surface was grind stepwise at a regular pitch distance of 0.5mm to reveal the marker across the billet height (Fig.1d). The geometry change of the markers was used as an index to quantify the strain distribution. The area lengths and average thicknesses of the markers in different layers were measured using ImageJ image processing software. Based on the geometry change, the true strain of the markers in the remnant billet was calculated according to the equations 1 to 5 specified by Li et al. [10]. By using the following equations, longitudinal strain, circumferential strain, radial strain, total strain, and effective strain were calculated at different depths of the billet.

$$\varepsilon_l = \ln\left(\frac{A_o}{A_n}\right) \quad (1)$$

$$\varepsilon_\theta = \ln\left(\frac{l_n}{d_o}\right) \quad (2)$$

$$\varepsilon_r = \ln\left(\frac{t}{d_o}\right) \quad (3)$$

$$\varepsilon_t = \varepsilon_l + \varepsilon_\theta + \varepsilon_r \quad (4)$$

$$\varepsilon_{eff} = \sqrt{(\varepsilon_l{}^2 + \varepsilon_\theta{}^2 + \varepsilon_r{}^2)} \quad (5)$$

Here $\varepsilon_l, \varepsilon_\theta, \varepsilon_r, \varepsilon_t$ and ε_{eff} are the longitudinal strain, circumferential strain, radial strain, total, and effective strain, respectively. A_0 is the original cross-sectional area of the marker, A_n is the area of the marker on a transverse cross-section. ln is the length of the marker in the circumferential (theta) direction, and d_0 is the original marker-wire diameter; t is the average thickness of the marker in the radial direction, and d_0 is the average chord of the original marker-wire diameter. By the definition of constant volume in continuum mechanics, the total strain ε_t, which is the sum of three mutually orthogonal strain components, the longitudinal strain, radial strain, and circumferential strain, should be zero. By plotting the strain values from the bottom to the top of the deformation zone, the strain evolution is revealed.

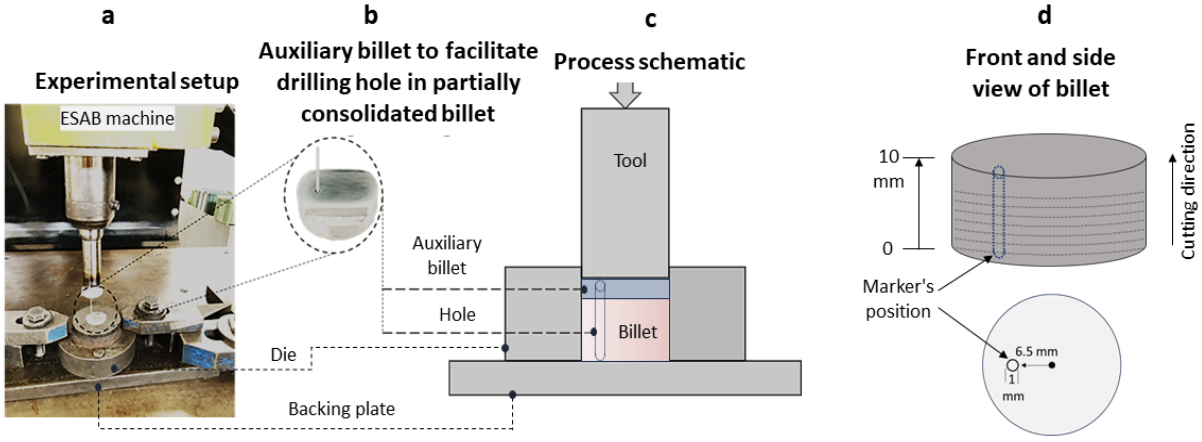

Fig. 1. Experimental setup and its schematic to analyze material flow during FSC process.

Materials Research Proceedings 44 (2024) 158-166 https://doi.org/10.21741/9781644903254-18

In order to further support the experimental results and get more insights into material flow during the FSC process, the numerical simulation was performed by using FEA commercial software DEFORM 3D. The tool, die and backing plate were modelled rigid bodies with a mesh size of 30000 elements while the billet of compacted chips was considered a porous object (25000 elements) with an embedded copper wire by implementing the Shima and Oyane [12] formulation on the mechanical properties definition of the material as depicted in Fig. 2. The inverse approach was adopted by setting suitable boundary conditions, in particular, constant friction equals to 0.4 and the heat transfer coefficient of 11 N/sec/mm/°C were considered.

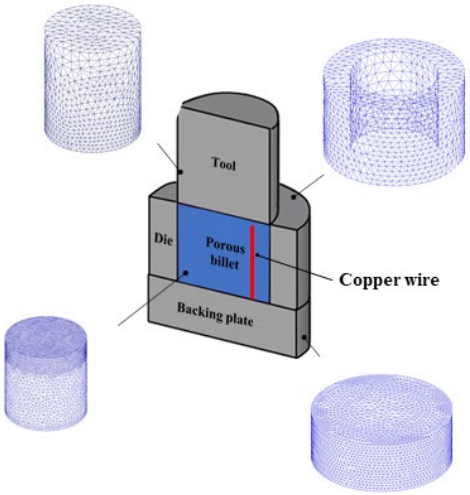

Fig. 2. Model for numerical simulation for material flow analysis.

Results

To visualize the deformation evolution and calculate the strain distribution during the deforming volume of FSC, the cross-sectional images of the AA7075 billet at different layers are presented in Fig. 3. Here, the bottom of the billet (contacting surface of billet and backing plate) was considered zero position Fig. 3. Each picture was labelled with the distance from the bottom of the billet. For example, 1 mm means the picture is taken from a cross section that is 1 mm above the bottom of the billet, in other words, 1 mm from the backing plate.

From the series of images, it is evident that no deformation was noticed at the bottom of the billet. However, the deformation occurred toward the top zone almost 3 mm below the top surface, or in other words the deforming zone is situated at a height between 7 mm and 10 mm from the bottom surface. As moving from the bottom surface towards the top, the marker starts to deform along the circumferential direction at a 7 mm distance till to the top surface. At the very top from 9 mm to 10 mm, the marker exhibited the highest deformation splitting and dispersing across the surface of the billet. It represents that this zone undergoes the highest strain during the FSC process.

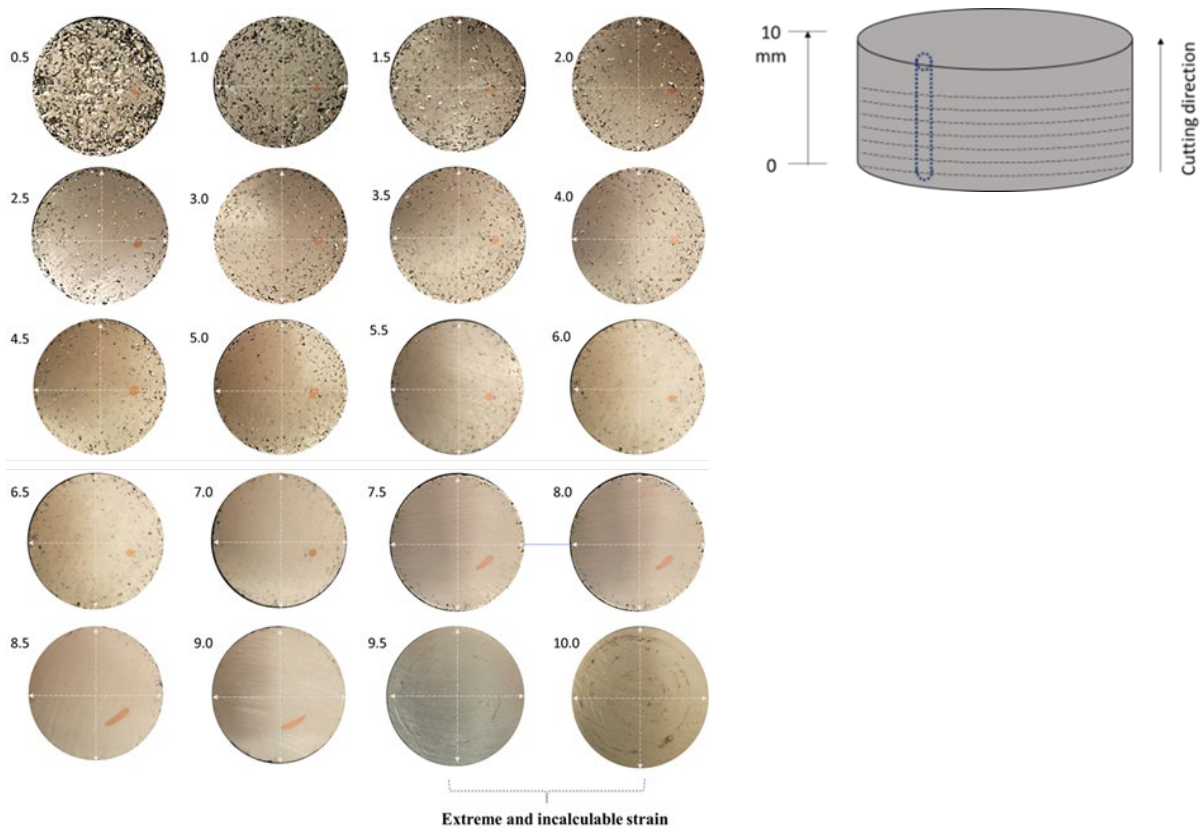

Fig. 3.Cross section of different layer of the FSC billet with respect its height.

The longitudinal strain (ε_l), circumferential strain (ε_θ), radial strain (ε_r), total strain (ε_t), and effective strain (ε_{eff}), at different depths in the deformation zone, are presented in Fig. 4. The circumferential strain increases from the position of 7 to 10 mm from the top of FSC billet and then decreases. The longitudinal strain is negative, and the absolute value continues to increase from the bottom to the top. It is important to note that the total strain is always close to zero, which indicates the obtained results are reliable. Based on the definition of the Von Mises effective strain in plasticity theory, see Eq. 5, effective strain (ε_{eff}) was calculated from three orthogonal strain components. That is, three mutually orthogonal strain components are not the principal strains. Plots of the calculated strain values were plotted with respect to their depths in the deformation zone shown in Fig. 4. As the top, most part (9-10 mm) underwent the highest strain, causing the marker to disperse across the billet section, the strain in this zone was incalculable.

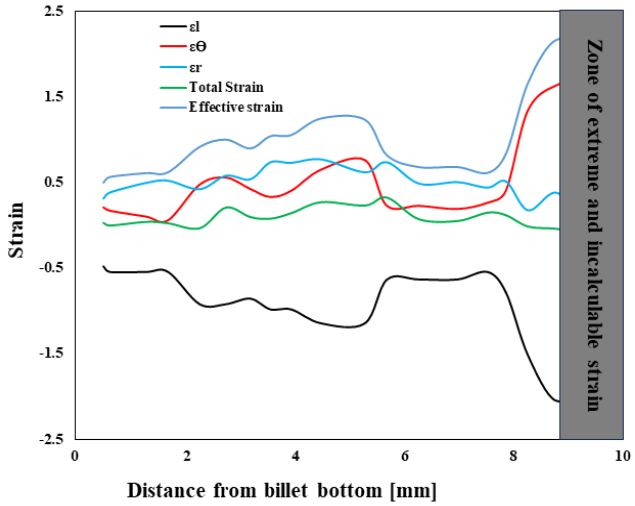

Fig. 4. Evolution of different strain across the FSC billet.

The simulation provides a qualitative overview of the material flow that characterizes the FSC process. At the end of the process, a point tracking and a flow net analysis were performed to emphasize the flow inside the porous billet. The flownet analysis has shown the flow in the entire cross section of the billet, while the horizontal point tracking was mainly added on the top surface of the billet to highlight how this surface moves during the FSC process (Fig. 5).

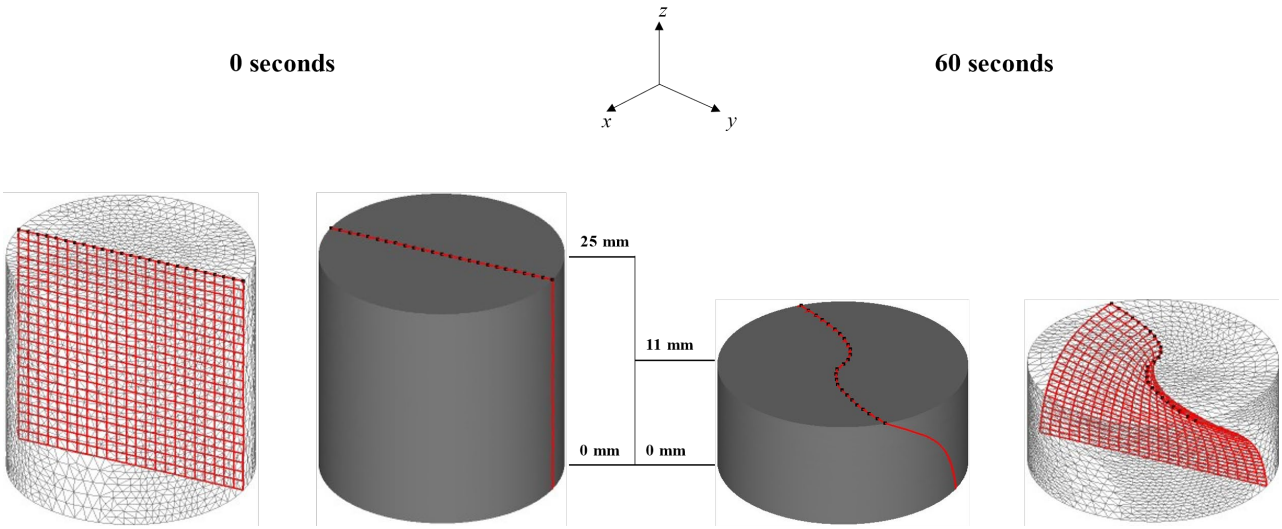

Fig. 5. Graphical visualization of the flownet (red grid) and the point tracking (black points) at the start (0 s) and the end of the process (60 s).

Additional results of the first flow analysis are presented in Fig. 6 where the rotation of the top surface is described by means of the displacement of a straight line of points. It is clearly visible that starting from the initial height of the billet the surface rotated by an angle of about 45°. Fig. 6 also shows that, due to the process configuration, the material close to the rotational center of the tool is characterized by a simple upsetting condition whilst the material close to the die surface is characterized by the highest rotation. In the same way, it is possible to distinguish and divide the 3D consolidated billet into two main zones: high strain level zone and low strain level zone (Fig. 7 and Fig. 8).

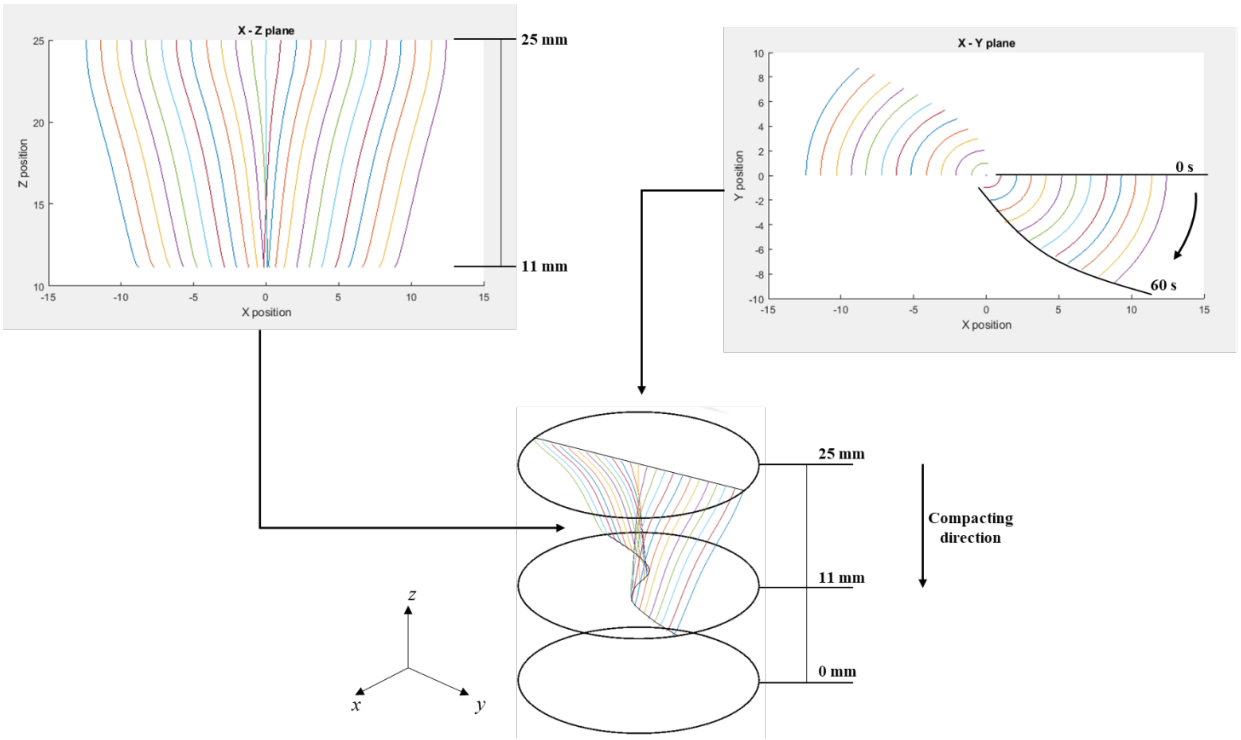

Fig 6. Point tacking visualization on MATLAB environment.

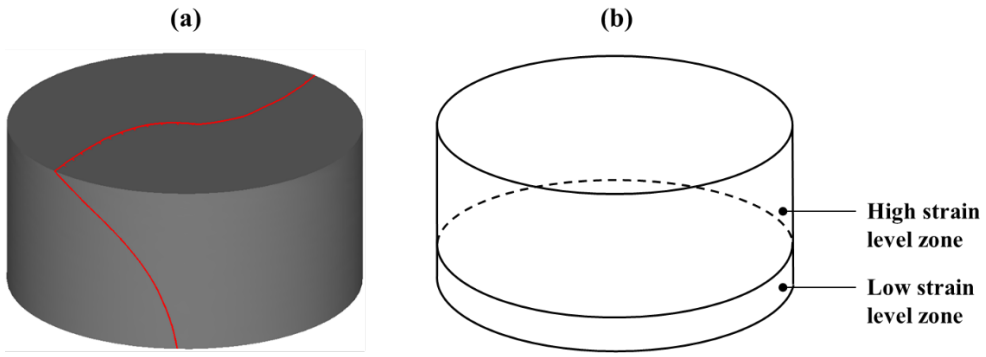

Fig. 7. (a) 3D view of the material flow and (b) two strain level zone division.

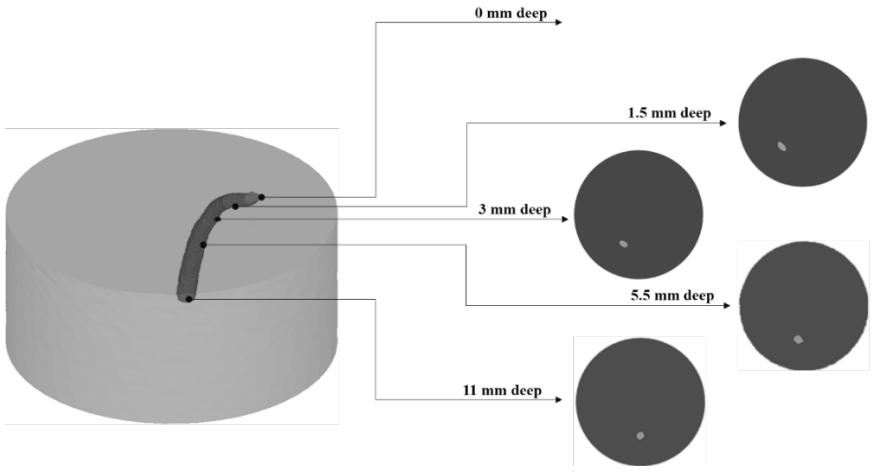

Fig. 8. Numerical acquisition of the wire surfaces at the end of the process, for different layers.

In order to further strengthen the arguments of the material flow occurrence at the top part and the absence of material flow at the bottom, the microstructure of the AA7075 consolidated billet was analyzed along its height at a radial distance of 6.5 mm as shown in Fig. 9. At the bottom of FSC billet, no significant change in the microstructure of the chips and bottom of the billet occurred. On the other hand, the formation of the new grain can be clearly seen at the top of the billet. These results depict that the bottom region is not affected by the strain and strain rate while it is expected that the top region is influenced by the combined effect of temperature, strain, and strain rate.

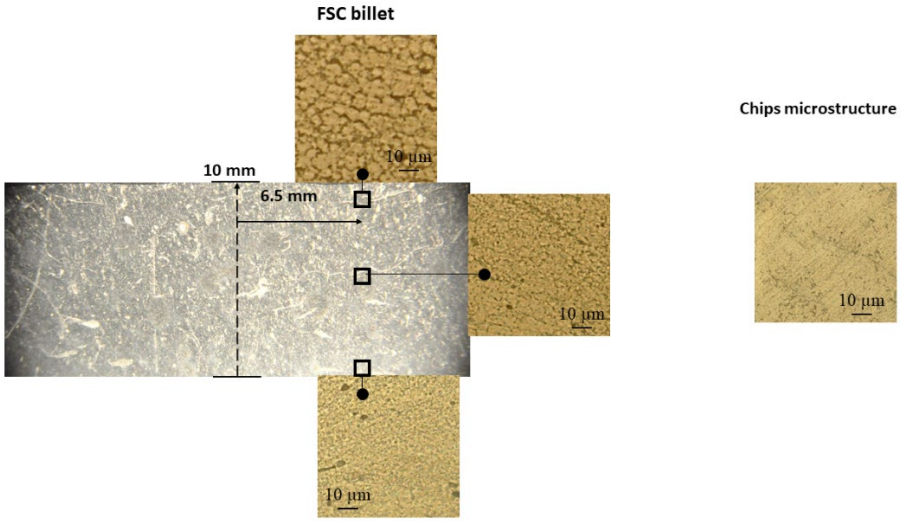

Fig. 9. Microstructure changes with respect to height of the FSC billet.

Conclusion

Although this study provided just a preliminary overview of the material flow during the FSC process. However, based on the previous discussion, the following conclusion can be drawn.
This study set up an experimental approach that depicted the material flow during the FSC of the AA7075 billet.

This research also will provide an effective avenue for obtaining the necessary strain values for establishing theoretical and numerical models for the FSC process.

In particular, the material flow occurred especially at the top zone of the billet, particularly in the zone between the top surface of the billet and 3 mm below.

The future work can be focused on improving the experimental setup for analyzing the material flow analysis, understanding the influence of the process parameters, and providing an improved numerical model to support material flow analysis results from the experimental data.

Acknowledgements

This study was carried out within the MICS (Made in Italy – Circular and Sustainable) Extended Partnership and received funding from the European Union Next-Generation EU (PIANO NAZIONALE DI RIPRESA E RESILIENZA (PNRR) – MISSIONE 4 COMPONENTE 2, INVESTIMENTO 1.3 – D.D. 1551.11-10-2022, PE00000004). This manuscript reflects only the authors' views and opinions, neither the European Union nor the European Commission can be considered responsible for them.

References

[1] D. Raabe, D. Ponge, P.J. Uggowitzer, M. Roscher, M. Paolantonio, C. Liu, H. Antrekowitsch, E. Kozeschnik, D. Seidmann, B. Gault, F. De Geuser, A. Deschamps, C.

Hutchinson, C. Liu, Z. Li, P. Prangnell, J. Robson, P. Shanthraj, S. Vakili, C. Sinclair, S. Pogatscher, Making sustainable aluminum by recycling scrap: The science of “dirty” alloys, Progress Mater. Sci. (2022) 100947. https://doi.org/10.1016/j.pmatsci.2022.100947

[2] J.R. Dufou, A.E. Tekkaya, M. Haase, T. Welo, K. Vanmeensel, K. Kellens, W. Dewulf, D. Paraskevas, Environmental assessment of solid state recycling routes for aluminium alloys: can solid state processes significantly reduce the environmental impact of aluminium recycling?, CIRP Ann. 64 (2015) 37–40. https://doi.org/10.1016/j.cirp.2015.04.051

[3] S. Shamsudin, M.A. Lajis , Z.W. Zhong, Evolutionary in solid state recycling techniques of aluminium: a review, Procedia CIRP 40 (2016) 256-261. https://doi.org/10.1016/j.procir.2016.01.117

[4] D. Baffari, A.P. Reynolds, A. Masnata, L. Fratini, G. Ingarao, Friction stir extrusion to recycle aluminum alloys scraps: Energy efficiency characterization, J. Manuf. Process. 43 (2019) 63-69. http://dx.doi.org/10.1016/j.jmapro.2019.03.049

[5] J.B. Jordon, P.G. Allison, B.J. Phillips, D.Z. Avery, R.P. Kinser, L.N. Brewer, K. Doherty, Direct recycling of machine chips through a novel solid-state additive manufacturing process, Mater. Design 193 (2020) 108850. https://doi.org/10.1016/j.matdes.2020.108850

[6] A. Latif, G. Ingarao, M. Gucciardi, L. Fratini, A novel approach to enhance mechanical properties during recycling of aluminum alloy scrap through friction stir consolidation, Int. J. Adv. Manuf. Tech. 119 (2022) 1989-2005. https://link.springer.com/article/10.1007%2Fs00170-021-08346-y

[7] L. Fratini, G. Buffa, D. Palmeri, J. Hua, R. Shivpuri, Material flow in FSW of AA7075–T6 butt joints: numerical simulations and experimental verifications, Sci. Tech. Weld. Join. 11 (2006) 412-421. https://doi.org/10.1179/174329306X113271

[8] T.U. Seidel, A.P. Reynolds, Visualization of the material flow in AA2195 friction-stir welds using a marker insert technique, Metall. Mater. Trans. A 32 (2001) 2879-2884. https://doi.org/10.1007/s11661-001-1038-1

[9] G.G. Stubblefield, K.A. Fraser, T.W. Robinson, N. Zhu, R.P. Kinser, J.Z. Tew, B.T. Cordle, J.B. Jordon, P.G. Allison, A computational and experimental approach to understanding material flow behavior during additive friction stir deposition (AFSD), Computat. Part. Mech. 1-15 (2023). https://ui.adsabs.harvard.edu/link_gateway/2023CPM....10.1629S/doi:10.1007/s40571-023-00578-x

[10] X. Li, M.R.E. Rabby, M. Ryan, G. Grant, A.P. Reynolds. Evaluation of orthogonal strain components in friction extrusion, J. Mater. Res. Tech. 15 (2021) 3357-3364. https://doi.org/10.1016/j.jmrt.2021.10.001

[11] T. Wei, A.P. Reynolds, Friction consolidation of aluminum chips, Friction Stir Weld. Process. VI (2011) 289-298. http://dx.doi.org/10.1002/9781118062302.ch34

[12] S. Shima, M. Oyane, Plasticity theory for porous metals, Int. J. Mech. Sci. 18 (1976) 285–291. https://doi.org/10.1016/0020-7403(76)90030-8